Supporting Information

Electrochemical Investigations into Kinase-Catalyzed Transformations of tau Protein

Meghan K. Rains[†], Sanela Martić[†,‡], Daniel Freeman[†], and Heinz Bernhard Kraatz[†]*

[†]Department of Physical and Environmental Sciences, University of Toronto Scarborough, 1265 Military Trail, Toronto, ON, M1C1A4, Canada; Department of Chemistry, University of Toronto, 80 St. George St., Toronto, ON, M5S3H6 Canada.

[‡]Department of Chemistry, Oakland University, 2200 North Squirrel Road, Rochester, MI, 48309, USA

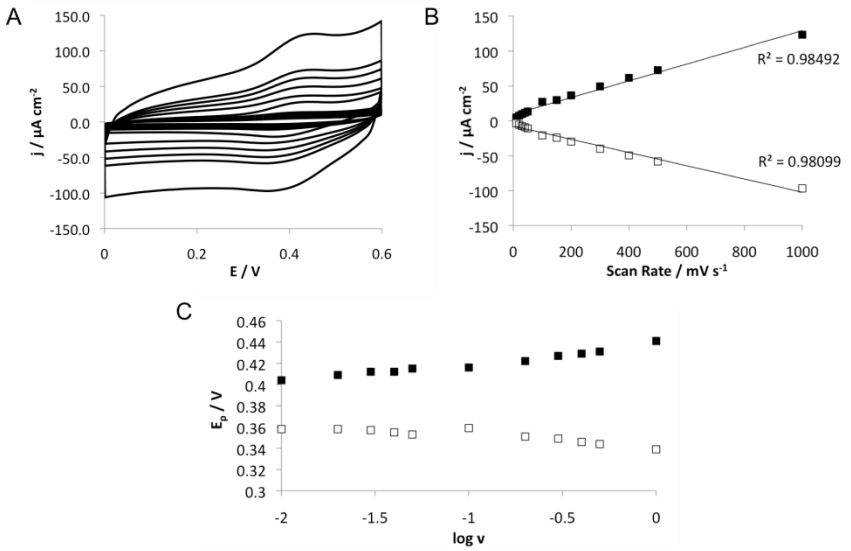

Figure S1. A) Cyclic voltammograms as a function of increasing scan rate for Fc-phosphorylated tau immobilized on a gold electrode. B) Plot of anodic and cathodic current densities as a function of scan rate. C) Laviron plot (log ν versus E_p) of the Fc-phosphorylated tau immobilized on gold electrode. (Src catalyzed Fc-phosphorylation, Ag/AgCl as reference electrode, Pt wire as auxiliary electrode, 2 M sodium perchlorate buffer pH 6.1).

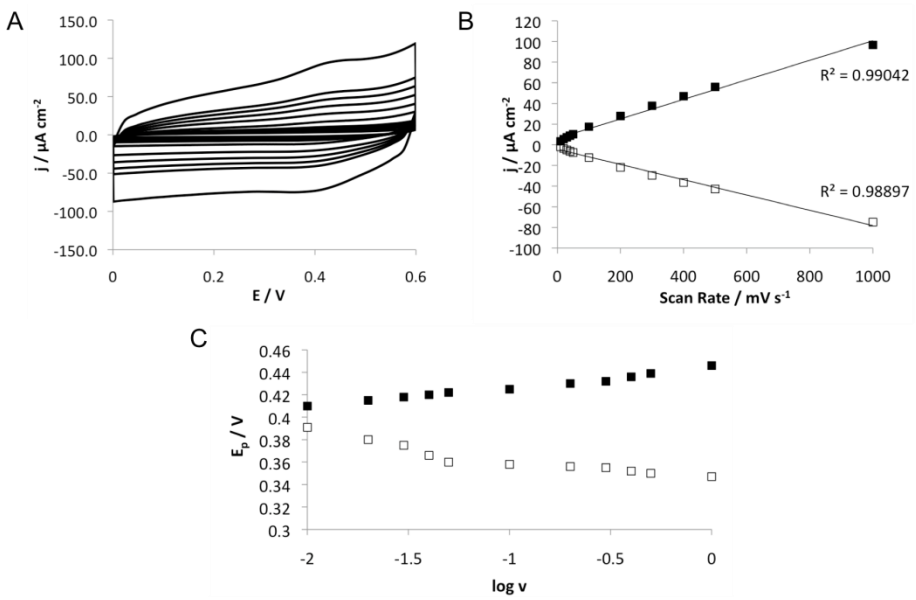

Figure S2. A) Cyclic voltammograms as a function of increasing scan rate for Fc-phosphorylated Tau immobilized on a gold electrode. B) Plot of anodic and cathodic current densities as a function of scan rate. C) Laviron plot (log ν versus E_p) of the Fc-phosphorylated Tau immobilized on gold electrode. (Src then Gsk-3β catalyzed Fc-phosphorylation, Ag/AgCl as reference electrode, Pt wire as auxiliary electrode, 2 M sodium perchlorate buffer pH 6.1)

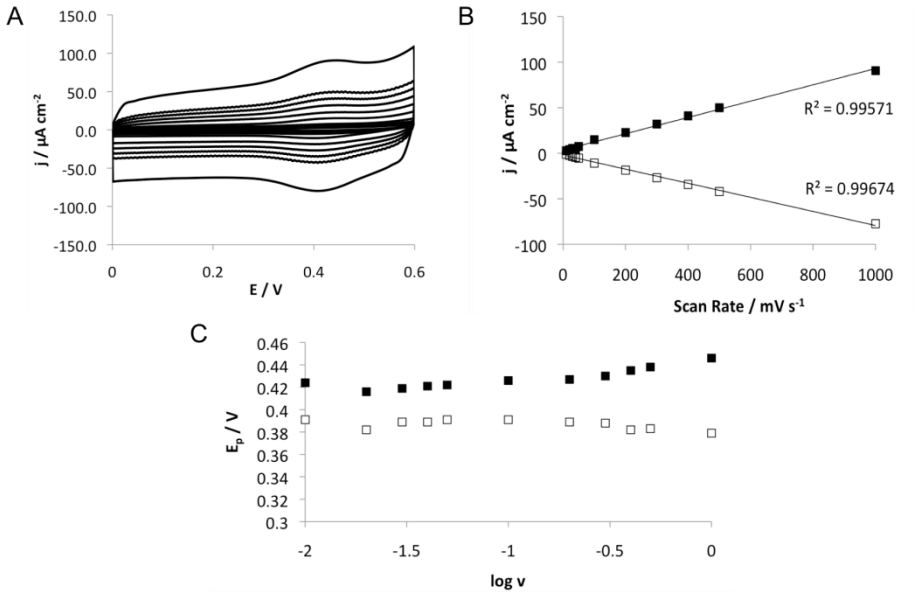

Figure S3. A) Cyclic voltammograms as a function of increasing scan rate for Fc-phosphorylated Tau immobilized on a gold electrode. B) Plot of anodic and cathodic current densities as a function of scan rate. C) Laviron plot (log ν versus E_p) of the Fc-phosphorylated Tau immobilized on gold electrode. (Abl catalyzed Fc-phosphorylation, Ag/AgCl as reference electrode, Pt wire as auxiliary electrode, 2 M sodium perchlorate buffer pH 6.1)

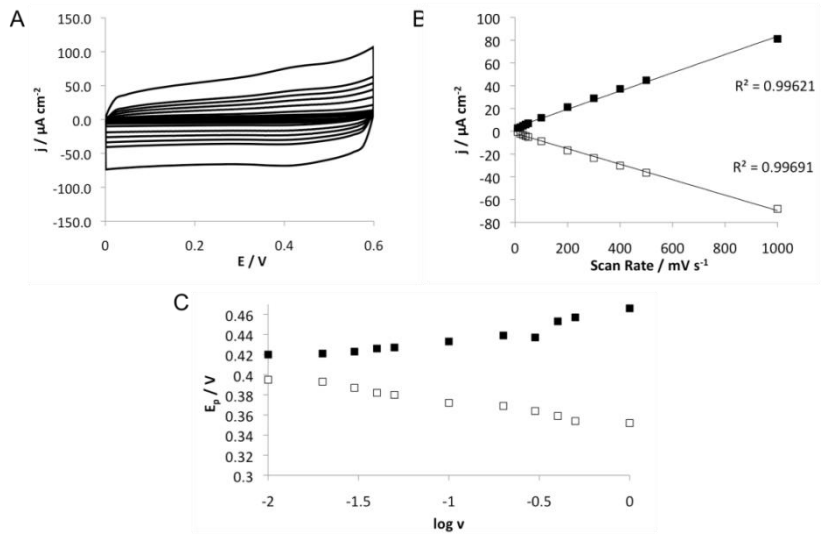

Figure S4. A) Cyclic voltammograms as a function of increasing scan rate for Fc-phosphorylated Tau immobilized on a gold electrode. B) Plot of anodic and cathodic current densities as a function of scan rate. C) Laviron plot (log ν versus E_p) of the Fc-phosphorylated Tau immobilized on gold electrode. (Abl then Gsk-3β catalyzed Fc-phosphorylation, Ag/AgCl as reference electrode, Pt wire as auxiliary electrode, 2 M sodium perchlorate buffer pH 6.1)

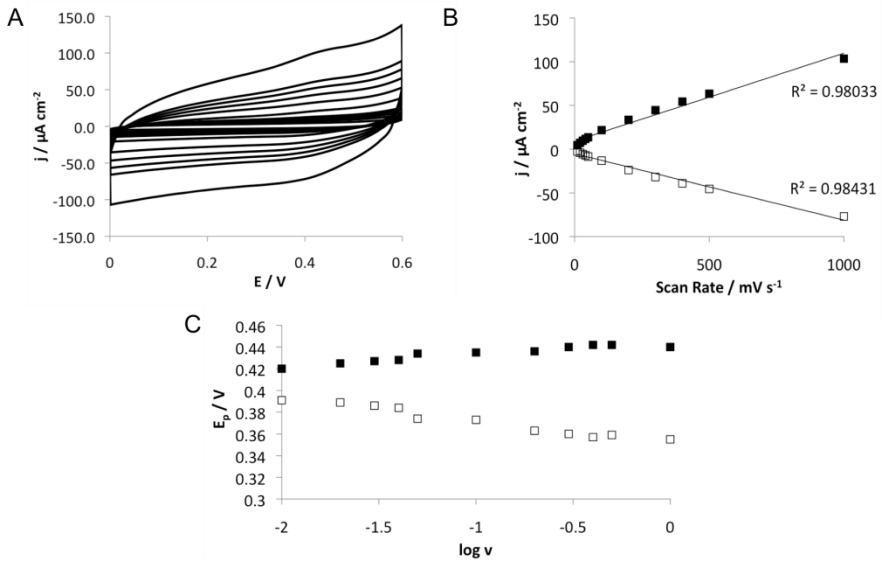

Figure S5. A) Cyclic voltammograms as a function of increasing scan rate for Fc-phosphorylated Tau immobilized on a gold electrode. B) Plot of anodic and cathodic current densities as a function of scan rate. C) Laviron plot (log ν versus E_p) of the Fc-phosphorylated Tau immobilized on gold electrode. (TTBK catalyzed Fc-phosphorylation, Ag/AgCl as reference electrode, Pt wire as auxiliary electrode, 2 M sodium perchlorate buffer pH 6.1

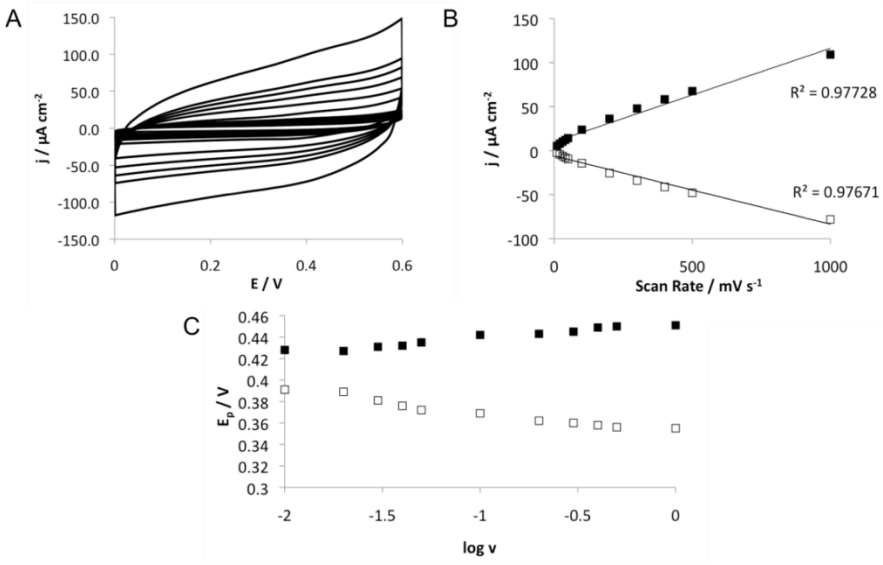

Figure S6. A) Cyclic voltammograms as a function of increasing scan rate for Fc-phosphorylated Tau immobilized on a gold electrode. B) Plot of anodic and cathodic current densities as a function of scan rate. C) Laviron plot (log ν versus E_p) of the Fc-phosphorylated Tau immobilized on gold electrode. (TTBK then Gsk-3β catalyzed Fc-phosphorylation, Ag/AgCl as reference electrode, Pt wire as auxiliary electrode, 2 M sodium perchlorate buffer pH 6.1)

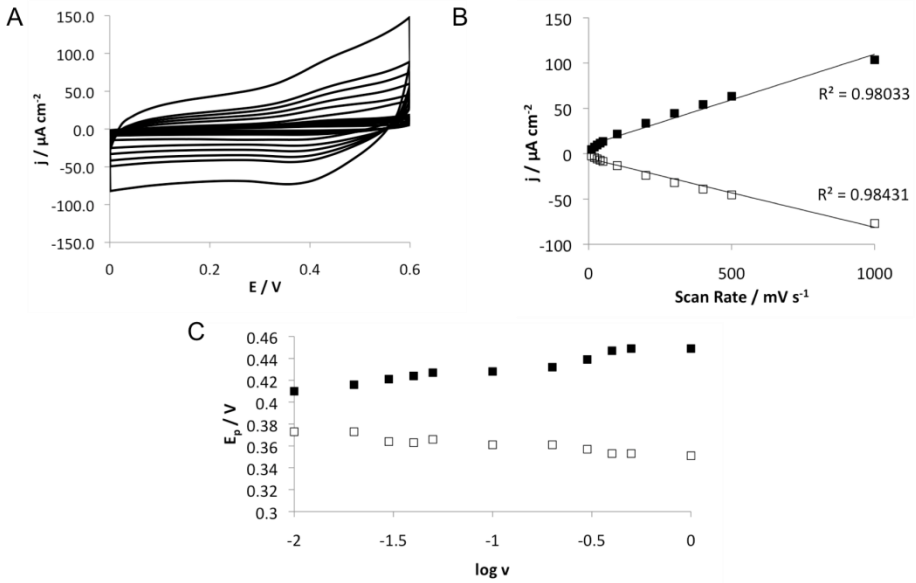

Figure S7. A) Cyclic voltammograms as a function of increasing scan rate for Fc-phosphorylated Tau immobilized on a gold electrode. B) Plot of anodic and cathodic current densities as a function of scan rate. C) Laviron plot (log ν versus E_p) of the Fc-phosphorylated Tau immobilized on gold electrode. (Fyn catalyzed Fc-phosphorylation, Ag/AgCl as reference electrode, Pt wire as auxiliary electrode, 2 M sodium perchlorate buffer pH 6.1)

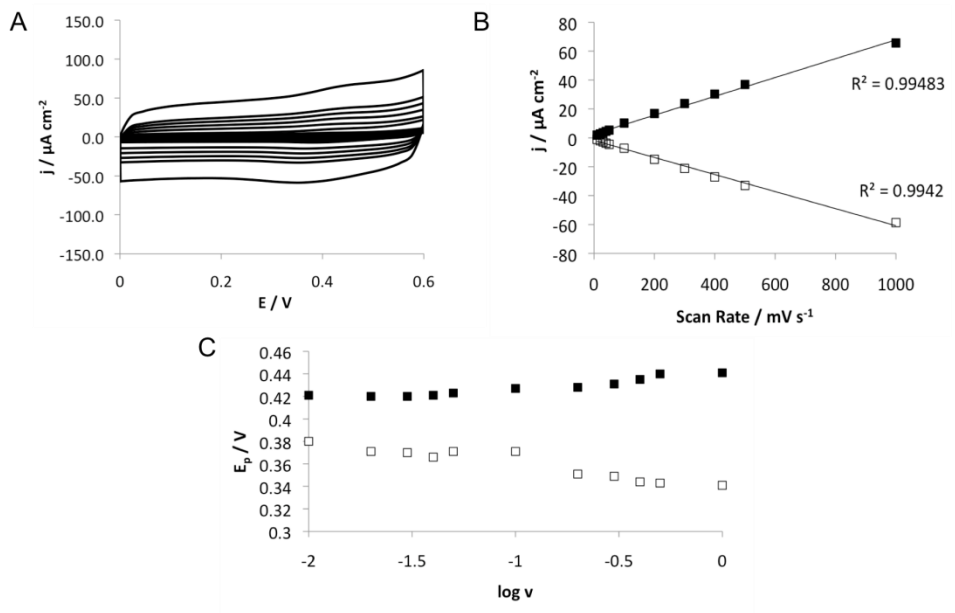

Figure S8. A) Cyclic voltammograms as a function of increasing scan rate for Fc-phosphorylated Tau immobilized on a gold electrode. B) Plot of anodic and cathodic current densities as a function of scan rate. C) Laviron plot (log ν versus E_p) of the Fc-phosphorylated Tau immobilized on gold electrode. (Fyn then Gsk-3β catalyzed Fc-phosphorylation, Ag/AgCl as reference electrode, Pt wire as auxiliary electrode, 2 M sodium perchlorate buffer pH 6.1)

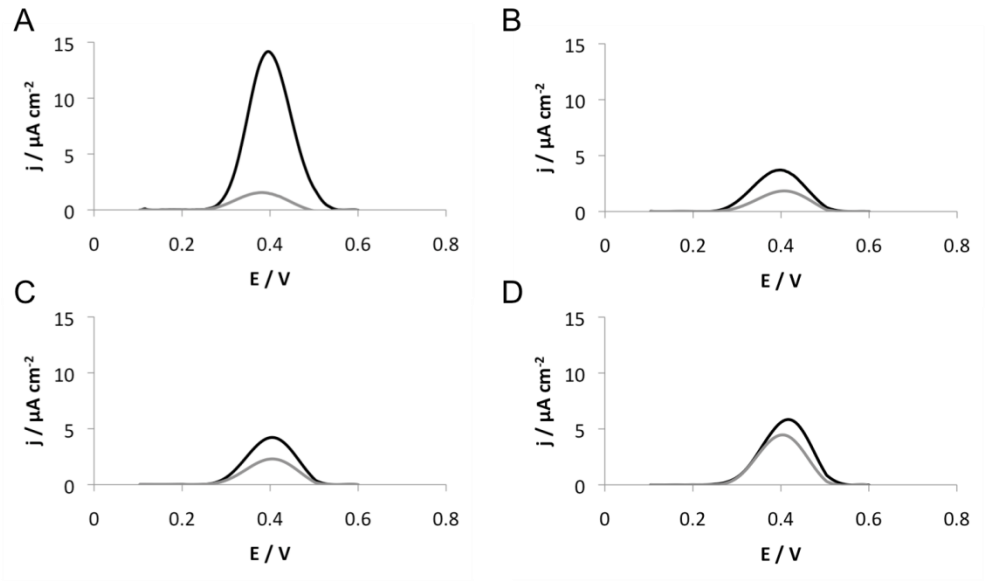

Figure S9. Background-subtracted square-wave voltammograms of Tau-modified gold electrodes after sequential Fc- phosphorylation reactions catalyzed first by tyrosine kinases (Black) then Gsk-3β (Grey) A) Src, B) Abl, C) TTBK, D) Fyn

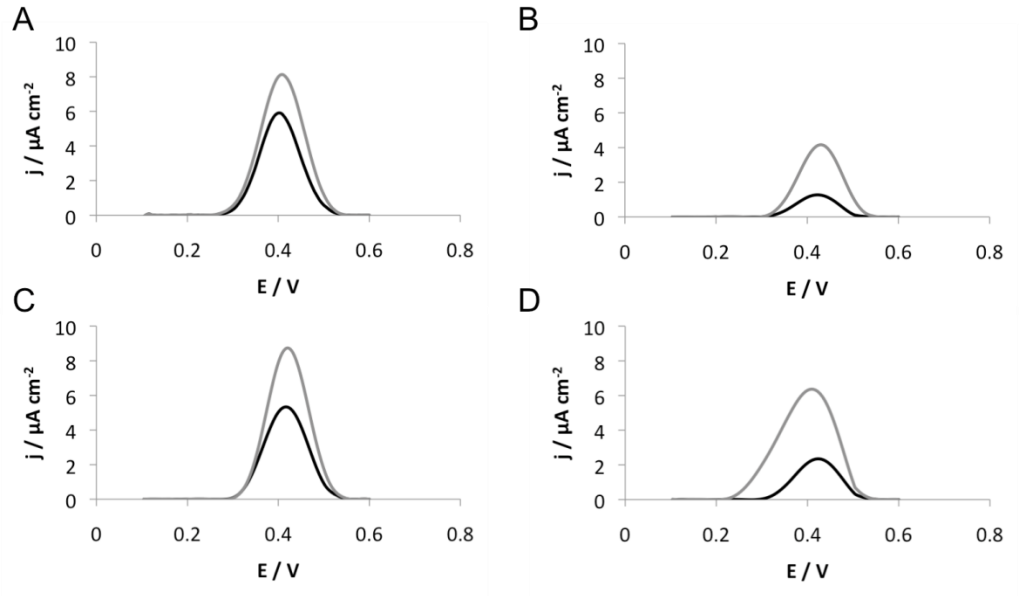

Figure S10. Background-subtracted square-wave voltammograms of Tau-modified gold electrodes after sequential Fc- phosphorylation reactions catalyzed first by Gsk-3β (Black) then tyrosine kinases (Grey) A) Src, B) Abl, C) TTBK, D) Fyn

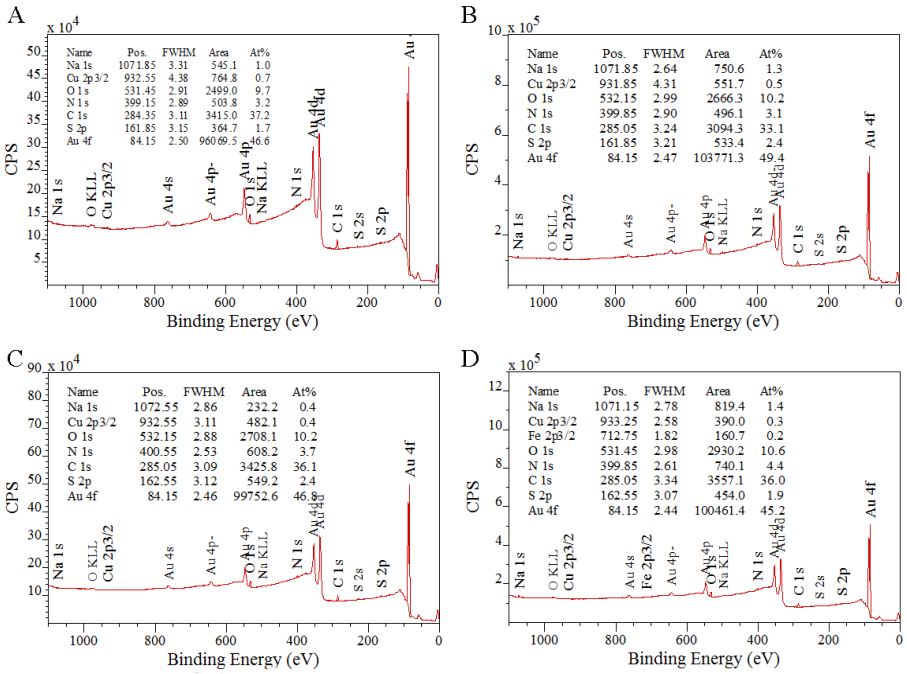

Figure S11. XPS survey spectra of tau films on gold surfaces following the Fc-phosphorylation reaction of immobilized tau in the presence of Fc-ATP and following protein kinases: A) Src, B) Src then GSK-3β, C) GSK-3β, and D) GSK-3β then Src.

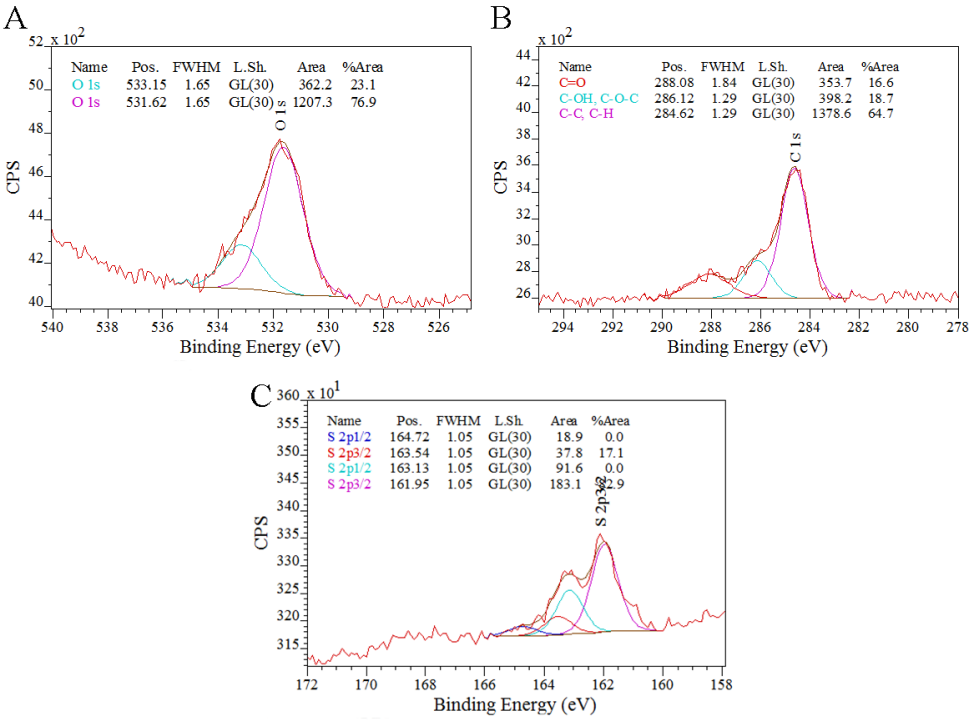

Figure S12. High resolution O 1s (A), C 1s (B), S 2p (C) XPS spectra of tau film on gold surfaces following the Fc-phosphorylation reaction of immobilized tau in the presence of Fc-ATP and Src protein kinase.

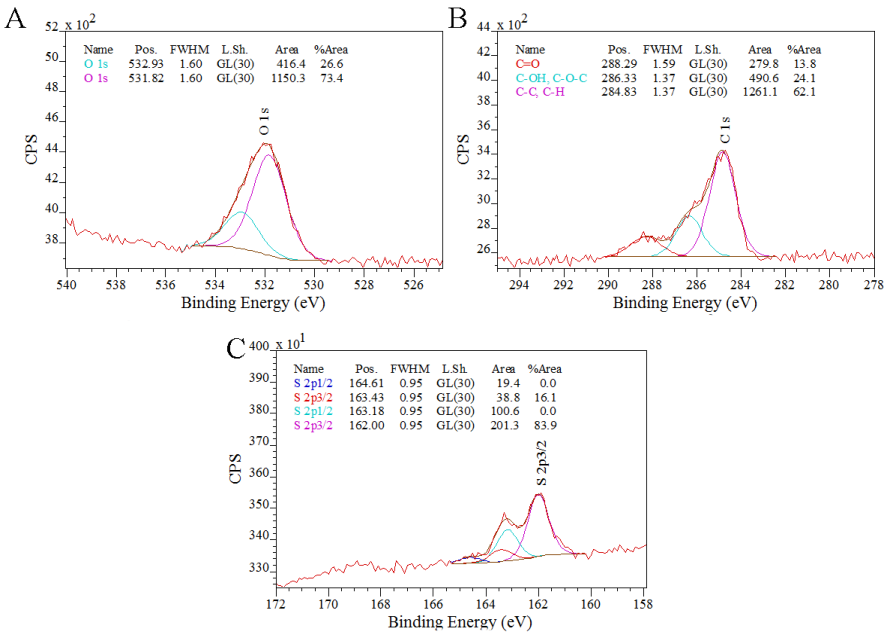

Figure S13. High resolution O 1s (A), C 1s (B), S 2p (C) XPS spectra of tau film on gold surfaces following the Fc-phosphorylation reaction of immobilized tau in the presence of Fc-ATP and Src followed by GSK-3β protein kinase.

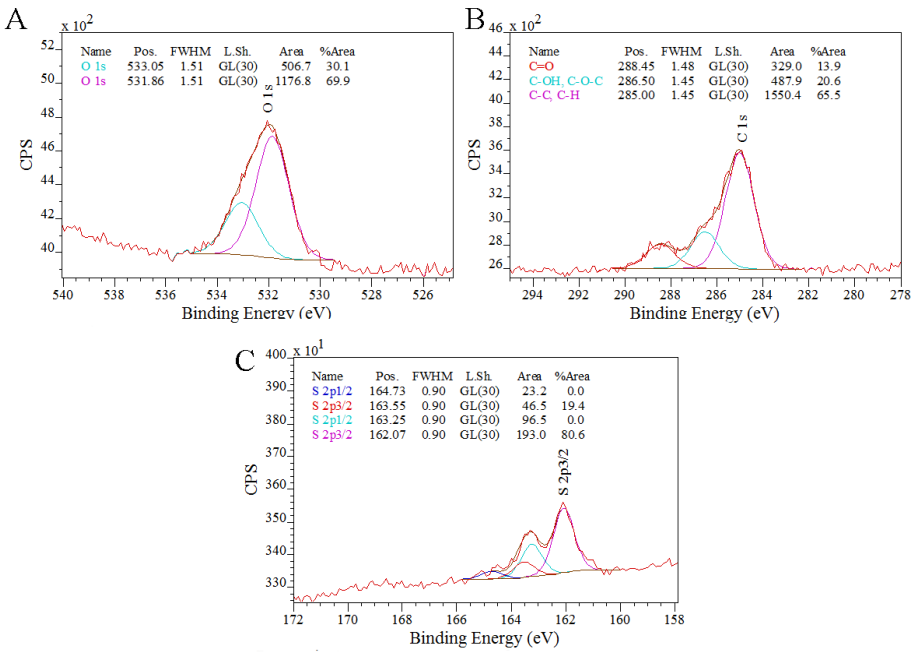

Figure S14. High resolution O 1s (A), C 1s (B), S 2p (C) XPS spectra of tau film on gold surfaces following the Fc-phosphorylation reaction of immobilized tau in the presence of Fc-ATP and GSK-3β protein kinase.

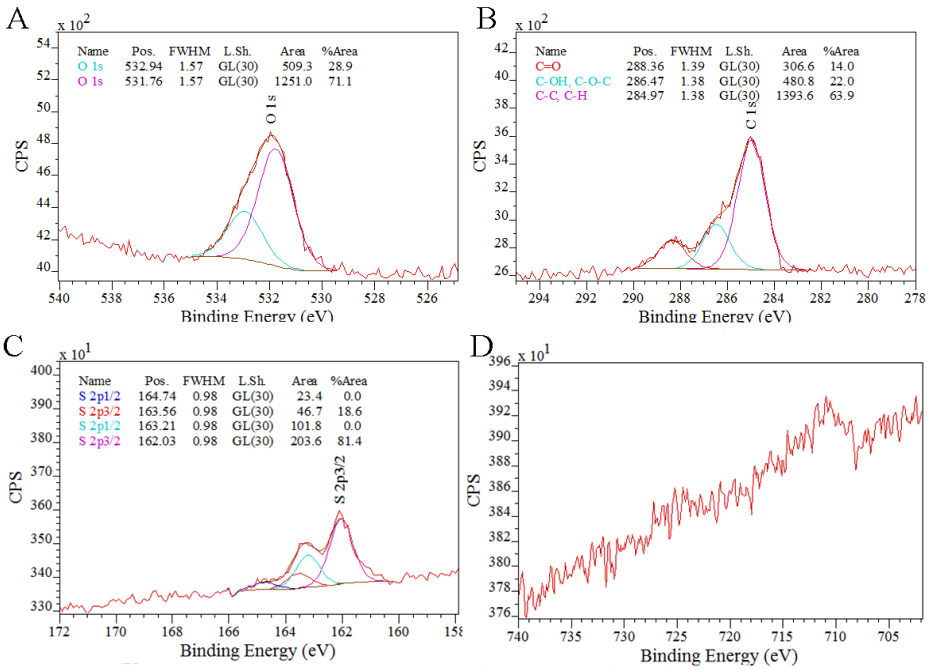

Figure S15. High resolution O 1s (A), C 1s (B), S 2p (C) XPS spectra of tau film on gold surfaces following the Fc-phosphorylation reaction of immobilized tau in the presence of Fc-ATP and GSK-3β followed by Src protein kinase

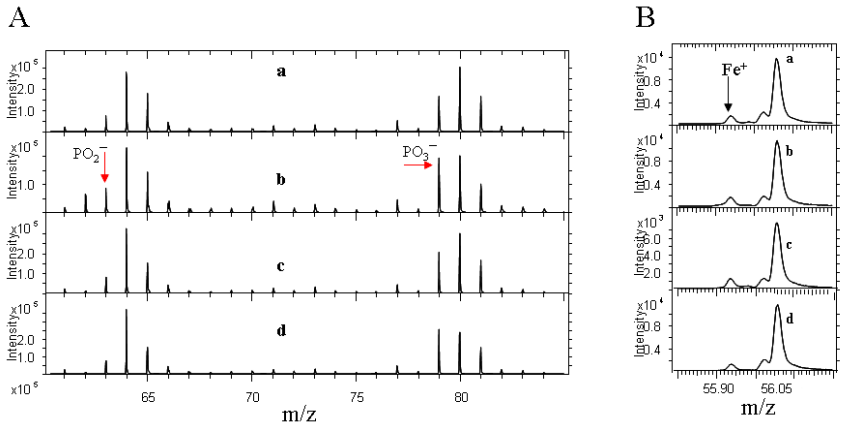

Figure S16. (A) Negative ion mode and (B) positive ion mode TOF-SIMS spectra of tau films on gold surfaces following the *in situ* Fc-phosphorylation of tau in solution in the presence of Fc-ATP and the following protein kinases: a) Src, b) GSK-3β, c) Src then GSK-3β, and d) GSK-3β then Src. Following the *in situ* reactions, the reaction mixture was immobilized on the lipoic acid N-succinimide active ster modified gold electrode. The ions of interest are PO_2^-, PO_3^-, and Fe^+ ions.

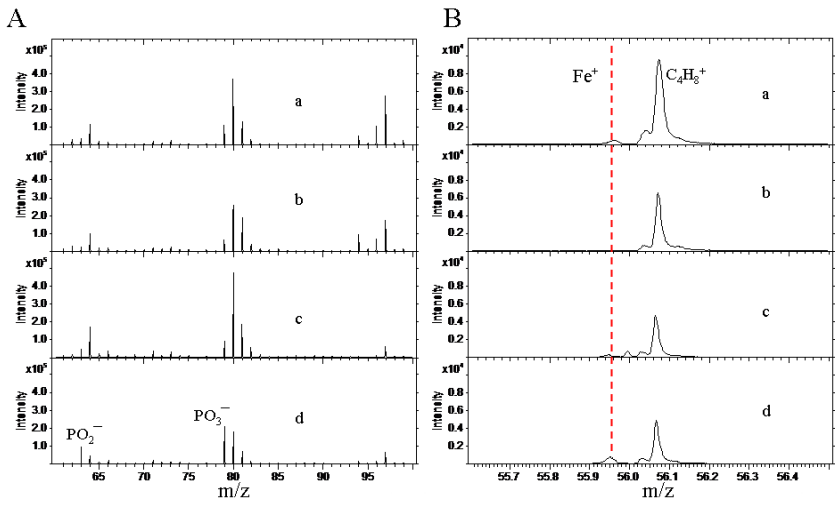

Figure S17. (A) Negative ion mode and (B) positive ion mode TOF-SIMS spectra of tau films on gold surfaces following the Fc-phosphorylation of immobilized tau in the presence of Fc-ATP and the following protein kinases: a) Src, b) Src then GSK-3β, c) GSK-3β, and d) GSK-3β then Src protein kinase. The ions of interest are PO_2^-, PO_3^-, and Fe^+ ions.

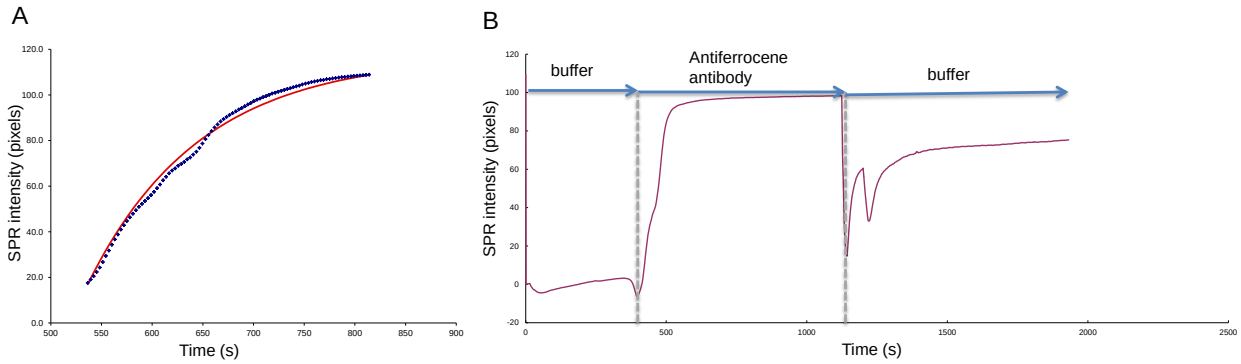

Figure S18. A) SPR data for antibody binding to Fc fit using first order exponential to determine k_{on} rate of Src catalyzed Fc-phosphorylation of tau on gold electrode and binding of antiferrocene antibodies. B) Full SPR spectrum of Src catalyzed Fc-phosphorylation of tau on gold electrode at different stages: buffer, antiferrocene antibodies, buffer.

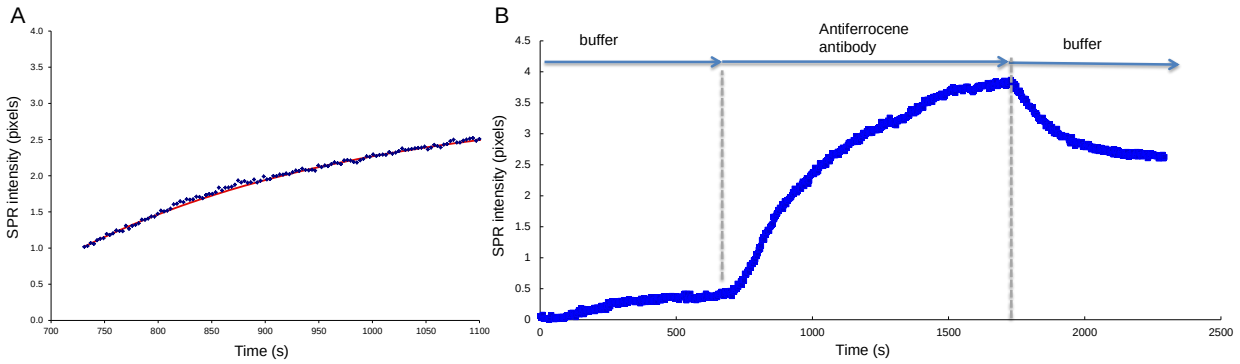

Figure S19. A) SPR data for antibody binding to Fc fit using first order exponential to determine k_{on} rate of Src then Gsk-3β catalyzed Fc-phosphorylation of tau on gold electrode and binding of antiferrocene antibodies. B) Full SPR spectrum of Src then Gsk-3β catalyzed Fc-phosphorylation of tau on gold electrode at different stages: buffer, antiferrocene antibodies, buffer.

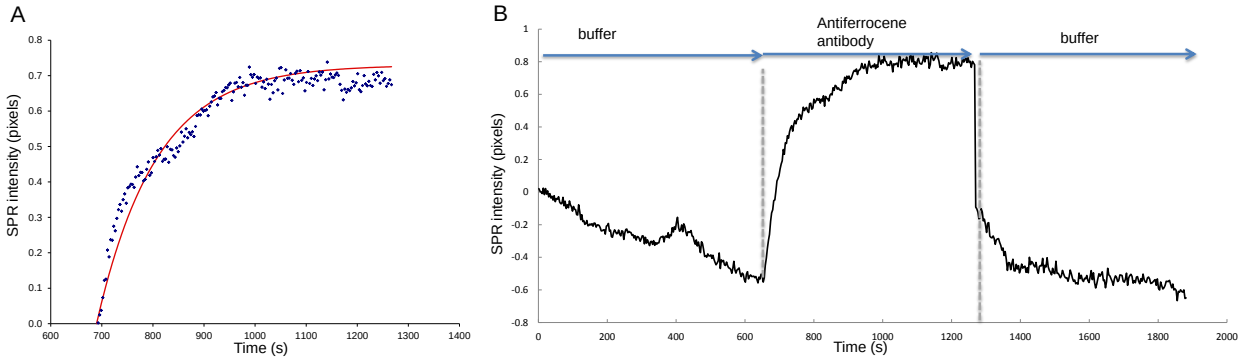

Figure S20. A) SPR data for antibody binding to Fc fit using first order exponential to determine k_{on} rate of Gsk-3β catalyzed Fc-phosphorylation of tau on gold electrode and binding of antiferrocene antibodies. B) Full SPR spectrum of Gsk-3β catalyzed Fc-phosphorylation of tau on gold electrode at different stages: buffer, antiferrocene antibodies, buffer.

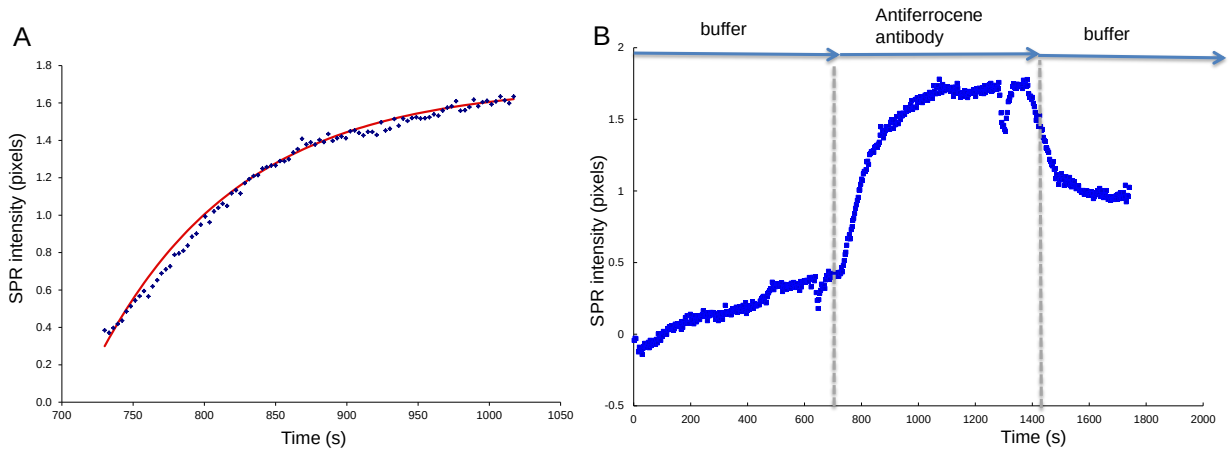

Figure S21. A) SPR data for antibody binding to Fc fit using first order exponential to determine k_{on} rate of Gsk-3β then Src catalyzed Fc-phosphorylation of tau on gold electrode and binding of antiferrocene antibodies. B) Full SPR spectrum of Gsk-3β then Src catalyzed Fc-phosphorylation of tau on gold electrode at different stages: buffer, antiferrocene antibodies, buffer.

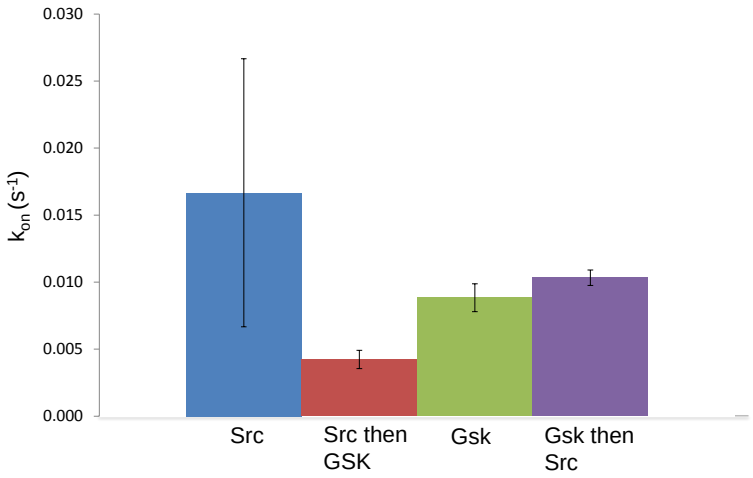

Figure S22. Plot of estimated k_{on} rate constants as a function of the Fc-phosphorylated tau films on gold electrode. The error bars represent the standard deviation associated with the triplicate measurements.

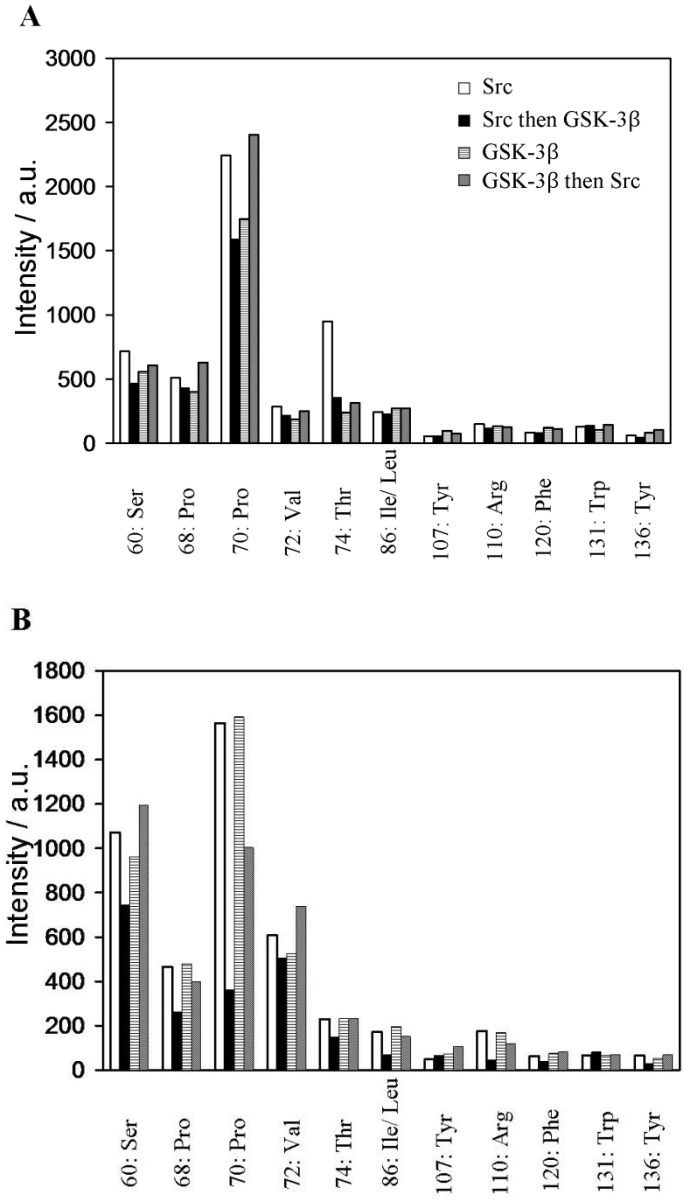

Figure S23. Plot of the positive ions intensities from TOF-SIMS spectra of different Fc-tau films prepared by A) surface-assisted Fc-phosphorylations and B) solution Fc-phosphorylations.

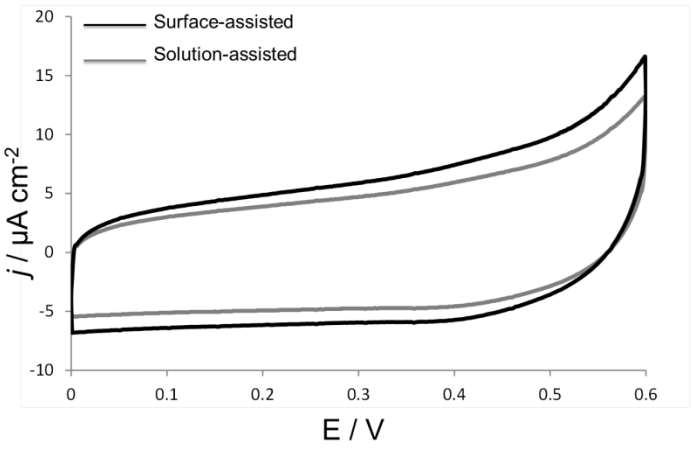

Figure S24. Cyclic voltammograms of reactions in the presence of FcATP but in the absence of protein kinase for the surface-assisted reaction with Tau immobilized on a gold electrode (——) and solution assisted reaction with Tau in solution which was subsequently immobilized on a gold electrode (——).

Table S1. Antibody binding kinetics determined for sequential Fc-phosphorylations of immobilized tau.

Kinase Used	k_{on}[a]
Src	9.0×10^{-3}
Src then Gsk-3β	3.7×10^{-3}
Gsk-3β	8.7×10^{-3}
Gsk-3β then Src	1.0×10^{-2}

[a] Rates reported as s^{-1} and fit using 1:1 binding model.

Table S2. Binding energy values (eV) and atomic percent (%) of S 2p, C 1s, N 1s, O 1s, and Fe 2p energy levels for various samples (N/A refers to the undetected energy levels).

Film	S 2p	C 1s	N 1s	O 1s	Fe 2p
Src	161.85	284.35	399.15	531.45	N/A
	1.7	37.2	3.2	9.7	
Src then GSK-3β	161.85	285.05	399.85	532.15	N/A
	2.4	33.1	3.1	10.2	
GSK-3β	162.55	285.05	400.55	532.15	N/A
	2.4	36.1	3.7	10.2	
GSK-3β then Src	162.55	285.05	399.85	531.45	712.75
	1.9	36.0	4.4	10.6	0.2